

Supplementary Information

System Modularity Chip for Analysis of Rare Targets (SMART-Chip): Liquid Biopsy Samples

Thilanga N. Pahattuge,^{a,b} Ian M. Freed,^{a,b} Mateusz L. Hupert,^c Swarnagowri Vaidyanathan,^{b,d} Katie Childers,^{b,d} Malgorzata A. Witek,^{a,b} Kumuditha Weerakoon-Ratnayake,^{a,b} Daniel Park,^{b,e} Anup Kasi,^f Mazin F Al-Kasspoles,^f Michael C. Murphy^{b,e} and Steven A. Soper
_{a,b,c,d,g,h}*

^aDepartment of Chemistry, University of Kansas, 1567 Irving Hill Rd, Lawrence, KS 66045, USA

^bCenter of BioModular Multi-scale Systems for Precision Medicine, University of Kansas, Lawrence, KS 66045, USA

^cBioFluidica, Inc., 1567 Irving Hill Rd, Lawrence, KS 66045, USA

^dDepartment of BioEngineering, University of Kansas, 1530 West 15th St, Lawrence, KS 66045, USA

^eDepartment of Mechanical & Industrial Engineering, Louisiana State University, 3261 Patrick F. Taylor Hall, Baton Rouge, LA 70803

^fDepartment of Medical Oncology, University of Kansas, Medical Center, Kansas City, KS, USA

^gDepartment of Mechanical Engineering, University of Kansas, 3138 Learned Hall, 1530 West 15th St, Lawrence, KS 66045, USA

^hDepartment of Cancer Biology and KU Cancer Center, University of Kansas, Medical Center, Kansas City, KS, USA

Corresponding Author

* Steven A. Soper, Department of Chemistry, University of Kansas, 1567 Irving Hill Rd, Lawrence, KS 66045, USA. Telephone: 785-864-3072; Email: ssoper@ku.edu

ORCID: 0000-0002-8292-7058

EXPERIMENTAL

Reagents and materials. COC (cyclic olefin copolymer) substrates (6013S-04) and COC cover plates (5013S-04, 250 μm) were purchased from TOPAS advanced polymers GmbH (Germany). PMMA (polymethyl methacrylate) substrates were obtained from SABIC Polymer Shapes (Raleigh, NC) and cover plates (250 μm) were purchased from Goodfellow (Oakdale, PA). Pt wires (75 μm diameter) were secured from Sigma Aldrich (St. Louis, MO) and gold-plated electrical contacts (09670008576) were purchased from Harting (Germany). PEEK tubing was obtained from IDEX Health & Science (Oak Harbor, WA). PEEK tubing interfaced to the motherboard were connected to syringe pumps (New Era, Farmingdale, NY) using Inner-Lock union capillary connectors (Polymicro Technologies) and barbed socket Luer Lock fittings (3/32" ID, McMaster-Carr). Solenoids (M1533724VDC) and a 12-station manifold (150M12) were purchased from Humphrey Products (Kalamazoo, MI) and PDMS membranes (HT6240, 250 μm) were secured from Standard Rubber Products Co. (Elk Grove Village, IL).

Chemical reagents used in this study included: Micro 90 (Cole-Palmer, Vernon Hills, IL), isopropyl alcohol (IPA), 1-ethyl-3-[3-dimethylaminopropyl] carbodiimide hydrochloride (EDC), N-hydroxysuccinimide (NHS), anhydrous acetonitrile (ACN), anhydrous triethyl amine (TEA; Sigma-Aldrich), phosphate buffered saline (PBS, pH 7.4), bovine serum albumin (BSA), 2-(4-morpholino)-ethane sulfonic acid (MES), nuclease free water (Fisher Scientific), and 1 M Tris pH 7.4 (KD Medical, Inc, Columbia, MD). Tris-glycine (TG) pH 8.3 was obtained from Bio-Rad (Hercules, CA). Hoechst 33342 and LIVE/DEAD Cell Imaging Kit were secured from Life Technologies.

The SKBR3 cell line was obtained from the American Type Culture Collection (ATCC). Culture reagents included fetal bovine serum (FBS, Performance, Gibco), McCoy's 5A (Corning), Trypsin (Sigma-Aldrich), and 25 cm² tissue culture flasks (Fisher Scientific). Mouse anti-human EpCAM/TROP-1 (clone 158210, 1 mg/mL), human EpCAM/TROP1 Alexa Fluor 488-conjugated antibody (clone 158206), Mouse IgG 2B Alexa Fluor 488-conjugated Isotype control (clone 133303) were from R&D Systems. Anti-CD45-FITC (Clone 2D1, 0.2 mg/mL) was purchased from eBiosciences (San Diego, CA) and Anti-Pan-Cytokeratin-Cy3 antibody (clone AE1/AE3, 0.2 mg/mL) was from Affymetrix Inc. (San Diego, CA). Blocking and washing buffers were filtered (0.2 μm, PTFE, Fisher Scientific) just prior to use.

Cell culture and antigen expression analysis. SKBR3 cells were cultured in 1× McCoy's 5A supplemented with 10% FBS at 37°C with 5% atmospheric CO₂. The cells were detached using trypsin, centrifuged at 300g for 5 min and resuspended in ice cold PBS before use.

Cells were washed with ice cold PBS three times and conjugated primary antibody (Alexa Fluor 488, h-EpCAM) was added (5-10 μl/10⁶ cells) to the suspension. The cell suspension was incubated in the dark for 30 min at room temperature following mixing. Unbound Abs were removed by washing the cells with 0.1% BSA/PBS three times. After each washing step, the cells were centrifuged (300g, 5 min), removal of the supernatant, and resuspended in buffer. Cells were filtered using non-sterile CellTrics filters (30 μm, Sysmex America, Inc, Lincolnshire, IL) and analyzed by flow cytometry (BD Accuri C6). Isotype Ab (Alexa Fluor 488, IgG 2B) was used as the control.

Fabrication of the modules and fluidic motherboard. The microfluidic components were manufactured via direct milling, hot embossing, and PDMS casting. The fluidic motherboard was

directly milled in PMMA using a Kern Evo high-precision micromilling machine (Kern Microtechnik GmbH, Germany) and FeatureCAM was used for the CNC programming. The CTC selection module and impedance module were prepared by hot embossing. Metal masters for hot embossing were prepared by micromilling a brass plate using high-precision micromilling with carbide bits (Performance Micro Tool) and the hot embossing was performed with a HEX03 embossing machine (Jenoptik GmbH). Hot embossing of the CTC selection module was performed in COC at 155°C with a 30 kN force applied for 120 s. Hot embossing of the impedance module in PMMA was conducted at 140°C with a force of 20 kN applied for 630 s. Embossed modules were diced with a bandsaw and cleaned by rinsing with 10% micro 90, IPA, and nano-pure water, and finally dried at 60°C for 30 min. Cover plates (254 μm) were cut, cleaned, and dried before use.

CTC selection module assembly. When assembling the CTC selection module, the cleaned modules and cover plates (COC) were exposed to UV/O₃ for 13 min (22 $\text{mW}\cdot\text{cm}^{-2}$, $\lambda = 254 \text{ nm}$) and then, the cover plate was placed on the embossed substrate. This assembly was placed between two borosilicate glass plates and clipped together followed by thermal fusion bonding at 134°C for 1 h.

Impedance module assembly. This module was assembled by placing platinum (Pt) electrodes ($d = 75 \mu\text{m}$) into electrode holding channels embossed into the substrate and UV/O₃ irradiating the cover plate and substrate (PMMA) for 10 min (22 $\text{mW}\cdot\text{cm}^{-2}$, $\lambda = 254 \text{ nm}$) with the electrodes in place. The module was finally assembled by placing the cover plate on top of the microchannels and thermal fusion bonding at 101°C for 15 min.

Imaging module. Reliefs for casting the imaging module consisted of an SU-8 photoresist on a Si wafer and prepared using standard lithographic procedures. Two optical masks were used for fabrication of the dual height relief structures.¹ An ~4 μm thick layer of SU-8 2005 photoresist was spun onto a Si wafer and after pre-exposure baking at 95°C for 3 min, the photoresist was exposed to UV radiation (MA6/BA6 Mask Aligner, Karl Suss; Germany) through an optical mask to produce the structures that would ultimately define the CTC retaining pores. After a post exposure bake at 95°C for 3 min, a second layer of SU-8 2050, 65 μm thick, was spun onto the top of the first photoresist layer. Following a pre-exposure bake at 95°C for 10 min, the second layer of photoresist was exposed to UV radiation using a different photomask to produce structures that would ultimately become the inlet and outlet fluidic channels. Active alignment was used during the second exposure step in order to assure proper alignment between the two SU-8 layers. A postexposure bake was performed using a temperature ramping procedure (25°C - 95°C at 7°/min, 95°C for 6 min and 95°C - 25°C at 1°/min) to minimize thermal stress in the SU-8 structures and improve adhesion to the Si wafer. Microstructures were then developed using SU-8 developer to form reliefs for PDMS casting.

Sylgard 184 (Dow Corning) was used for the imaging module. Following the manufacturer's procedure, a mixture containing 10:1 (w/w) PDMS prepolymer and curing agent was thoroughly stirred and degassed under vacuum, poured over the SU-8 microstructures, and into a custom-built retaining reservoir and cured at 75°C for 5 h in a natural convection oven. After removal from the casting master, single imaging modules were diced from the cast PDMS and inlet and outlet holes were punched into the substrate. The PDMS modules were then cleaned and dried and bonded to pre-cut glass slides following a 1 min exposure to O₂ plasma (90 W, 20 sccm O₂) in a reactor (Diener Electronic, GmbH + Co KG; Germany).

Surface attachment of monoclonal antibodies (mAbs) using photocleavable (PC) linkers. PC linker and mAb immobilization were recently reported by our group.² Briefly, assembled COC cell selection modules were UV/O₃ activated (22 mW·cm⁻², 13 min) and EDC (20 mg/mL) / NHS(2 mg/mL) treated for 25 min at room temperature using dry ACN. The solution was removed from the module by passing air, and PC linker (0.53 mM) dissolved in dry ACN and TEA was infused into the modules. After 2 h of incubation at room temperature, the solution was replaced by passing air through the module. Then, 100 mM Tris (pH 7.4) was introduced into the module and incubated for 30 min at room temperature. Next, Tris buffer was replaced by passing air and the EDC/NHS reaction was performed again. After incubation, the EDC/NHS solution was replaced with mAb (anti-EpCAM, 1 mg/mL) dissolved in PBS (pH 7.4) that was introduced into the module. The module was incubated for 2 h at room temperature or overnight at 4°C. Prior to sample infusion, the module was rinsed with 2 mL of 0.5% BSA/PBS at 50 μL/min to remove any unbound mAbs and minimize non-specific binding of sample components to the module's walls.

Microfabrication of the motherboard and membrane valve characterization. Fabrication of the membrane valves was reported previously.³ Briefly, the fluidic microchannels and pneumatic control channels (w × h, 760 μm × 180 μm), which were situated on the fluidic motherboard, were directly milled (Nomad 883, Torrance, CA) in two different PMMA substrates. The fluidic microchannel substrate also had the valve seats (400 μm) while the pneumatic control channels contained the displacement chambers (radius = 1400 μm). The two PMMA pieces were cleaned and dried. Channel measurements were made by using a VK-X 3D laser scanning confocal microscope (Keyence). The PMMA substrate with the fluidic microchannels and PDMS membrane (HT6240, 250 μm) were UV/O₃ treated (22 mW·cm⁻²) for 10 min. Next, the UV/O₃ exposed surfaces of the PDMS membrane was placed on top of the UV/O₃ exposed PMMA fluidic

microchannel surface and they were conformally bonded together. The PMMA/PDMS assembly was again UV/O₃ activated for 10 min along with the pneumatic control PMMA layer. The pneumatic control layer was placed on top of the PDMS membrane and pressure was applied (165 psi) using a PHI Precision Press (TS-21-H-C (4A)-5, City of Industry, CA) after properly aligning the fluidic and pneumatic control layers. PEEK tubing (1/32" and 1/16") was attached to make the final device.

Valve characterization was accomplished by measuring the outlet flow rate by varying forward fluidic pressures at valve-open and valve-closed states. The inlet of the valve was connected to a pressure sensor (15 psi) and to a fluidic channel (dye solution), which was connected to a compressed N₂ gas tank. The flow rate was measured by weighing the amount of dye solution flowed through the device in a given time interval. Valve operation was controlled by providing a vacuum (to open the valve) or pressure (to close the valve) through the pneumatic control layer. Flow rates were measured at valve-open states (-50 kPa valve open pressure; (-) sign indicates vacuum) and two valve-closed states (25 kPa or 35 kPa valve closing pressures).

Relationship between impedance signal polarity and cell viability. SKBR3 cells were suspended in 1× TG buffer and incubated for 1 h at room temperature. The cells were hydrodynamically introduced into the impedance module at 30 µl/min (200 µl) while recording the impedance signals. The cells flown through the impedance module were collected into a 96 well plate and centrifuged at 300g for 5 min. The supernatant was removed and ice-cold PBS was added. The cells were stained using a Live/dead cell kit (Life Technologies) and incubated for 15min at room temperature. Cells were observed using a Zeiss Axiovert 200M microscope with a 10X objective (0.3 NA, Plan NeoFluar), an XBO 75 W lamp, FITC and Cy3 filter set (Omega

Optical), a Cascade 1K EMCCD camera (Photometrics), and a MAC 5000 stage (Ludl Electronic

Products). All of the microscope components were computer-controlled via Micro-Manager. Calcein and Ethidium homodimer stained cells were counted and compared with the corresponding impedance signals.

Cell retention in imaging module. SKBR3 cells were stained with Calcein and incubated at room temperature for 15 min. Imaging modules (4, 6 and 8 μm pore sizes) were rinsed with 0.5%BSA/PBS at 20 $\mu\text{L}/\text{min}$ (500 μL). Cells were diluted (~ 2 cells/ μL) with PBS and hydrodynamically introduced into the imaging module at 20 $\mu\text{L}/\text{min}$ (100 μL) while collecting the effluent into a 96 well plate. The imaging module was rinsed with 0.5%BSA/PBS at 20 $\mu\text{L}/\text{min}$ (100 μL) while collecting the washing buffer into the same well and observed using a Zeiss Axiovert 200M microscope using the FITC filter cube of the epifluorescence microscope. The cells retained in the imaging module and present in the 96 well plate were then counted.

Patient samples. Patient samples were secured from KUMC according to the institution's IRB protocol. Written informed consent was obtained from the patient before enrollment. Blood samples were collected into Vacuette K3EDTA (Greiner) tubes containing the anticoagulant EDTA and 50 $\mu\text{g}/\text{mL}$ eptifibatide⁴ and processed in the SMART-Chip on the second day after blood withdrawal.

RESULTS AND DISCUSSION

Connecting modules to the motherboard. Selection of fluidic interconnects was based on such factors as manufacturability, production cost, ease of application, dead volume, and reliability.

Based on the required operational metrics, we selected interconnects composed of two conically shaped receiving ports molded/milled into the module and motherboard and a connector tube made from a semi-rigid polymer, Tefzel. Conical receiving ports of the motherboard were milled from the back of the PMMA substrate that had fluidic channels (**Figure S1A**) using a 3° bit. The conical receiving ports had a top diameter of 1.70 mm, bottom diameter of 1.44 mm, and depth of 2.2 mm (**Figure S1B**). Assembly involved inserting the Tefzel tubes into the receiving ports on the motherboard, aligning the module, and pressing the two parts together (**Figure S1C**). During the compression step, the semi-rigid connecting tube conformed to the conically shaped ports and provided a tight seal with minimal unswept volume. Permanent connection between the two pieces was provided by using an adhesive (**Figure S1D**). We successfully tested these interconnects to pressures up to 3 MPa without leakage. This type of interconnect is also self-aligning and did not require additional alignment features for proper placement of the modules on the motherboard, which simplified cartridge design and facilitated assembly.

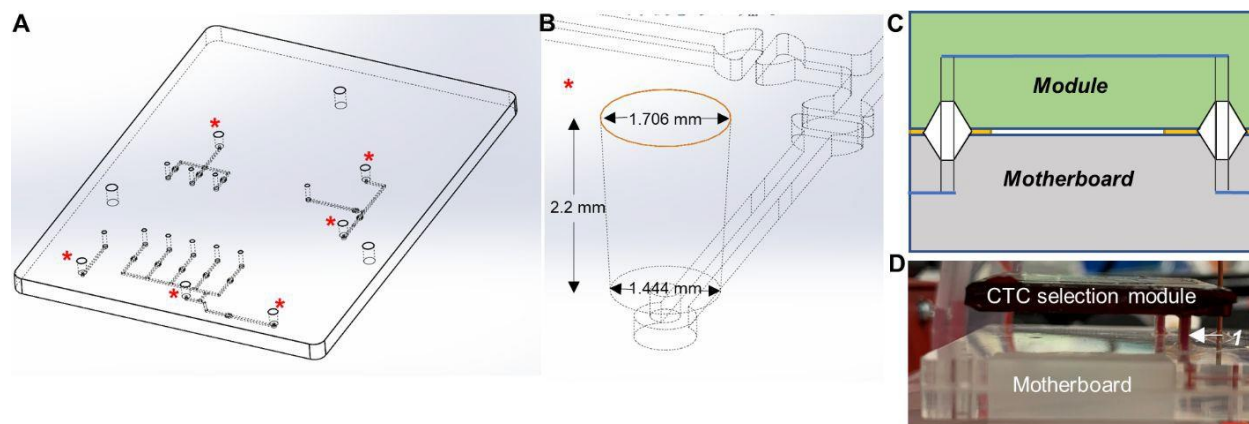


Figure S1. Task-specific module integration to the fluidic motherboard. (A) Conical receiving ports were milled from the back of the fluidic channel layer of the motherboard, where individual modules were connected (* marks the position of these ports on the motherboard). (B) The conical port had a top diameter of 1.706 mm and bottom diameter of 1.444 mm. Port depth was 2.2 mm for a 3.175 mm (1/8") thick substrate. (C) Schematic representation of fluidic interconnects for attaching modules to the motherboard. Conical receiving ports were molded into the modules. (D) Semi-rigid Tefzel tubing (1) was permanently bonded with an adhesive to make a leak-free connection with minimal unswept volume. The image was taken when processing a blood sample through the system.

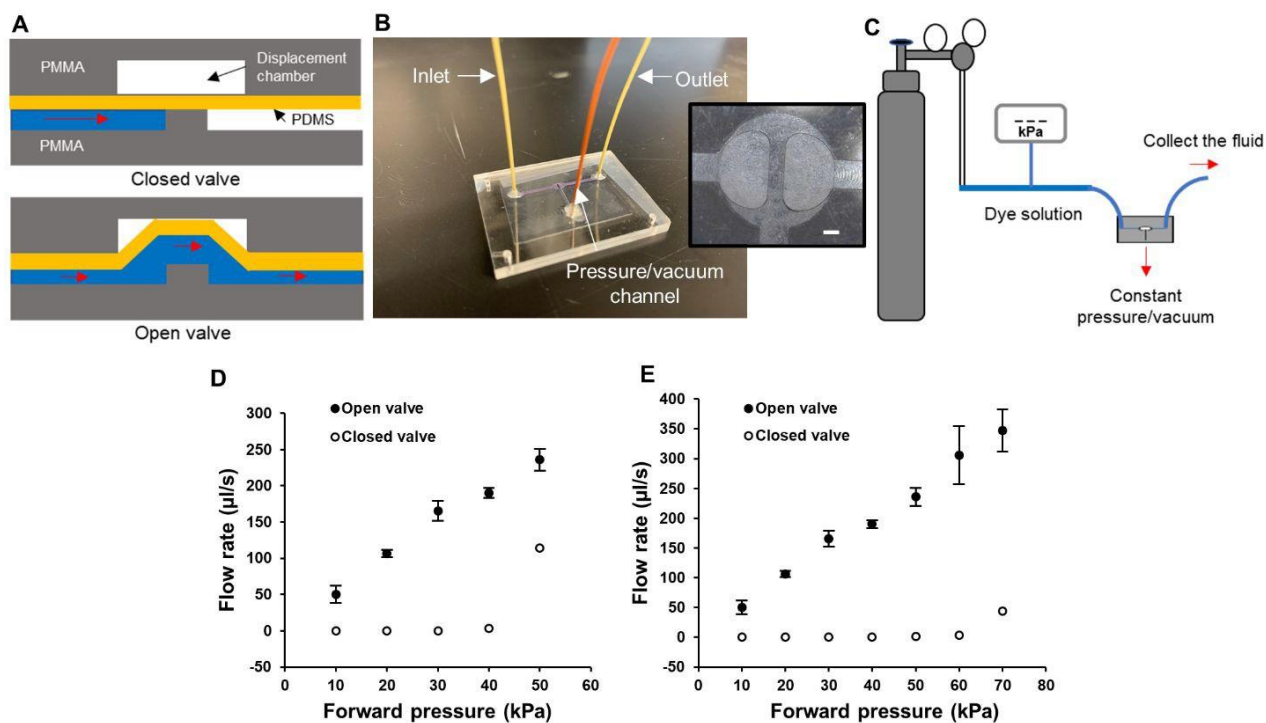


Figure S2. PMMA/PDMS/PMMA valve characterization. **(A)** The valve was normally closed. It was assembled by placing a UV/O₃ treated PDMS membrane (254 µm thick) between two UV/O₃ treated PMMA sheets that had fluidic and pneumatic channels. The valve can be opened by applying a vacuum through the pneumatic layer. **(B)** Pressure was applied to the PMMA/PDMS/PMMA layers to facilitate bonding and PEEK tubing was attached to make the final valve assembly. The scale bar is equivalent to 400 µm. **(C)** Schematic diagram of the valve characterization setup. The inlet of the valve was connected to a gas tank (N₂) via a dye solution filled tube and a pressure sensor. Outlet flow rate was measured by providing different forward pressures with a constant pressure (close-valve) or vacuum (open-valve) applied through the pneumatic control channels. **(D)** At 25 kPa pneumatic pressure (closed valve), the valve started leaking at 40 kPa forward pressure (n = 3). **(E)** When the pneumatic pressure was increased to 35 kPa (closed valve), the valve started leaking at 60 kPa forward pressure (n = 3).

Characterization of the microvalves. The membrane valves incorporated into the motherboard were first reported by the Mathies group³ with several modifications reported.⁵⁻⁶ The valves are normally closed and fabricated by sandwiching a thin PDMS membrane between two PMMA layers after UV/O₃ activation. The valve operation was controlled by applying a vacuum (open) or pressure (close) through pneumatic control channels via a computer-controlled solenoid system. At normal position and/or with a positive pressure, the PDMS membrane sits on the valve seat and prevents liquid passage. When a vacuum is applied, the PDMS membrane moves into the displacement chamber opening the valve (**Figure S2A**). We prepared a single valve for characterization

purposes. Fluidic and pneumatic control channels were directly milled into PMMA, which was used as the substrate. The PDMS membrane and two PMMA substrates were UV/O₃ treated and the microvalve was prepared by bonding the layers together (**Figure S2B**).

The performance of the valve was evaluated by measuring the outlet flow rate under different fluidic forward pressures at valve open and closed states. Different fluidic pressures were obtained by connecting the inlet of the valve to a gas cylinder and a tube filled with a dye solution (**Figure S2C**). When the valve was in the open state, the outlet flow rate increased linearly with forward fluid pressure (**Figure S2D-E**, black dots). When a pressure was applied through the pneumatic control channel to close the valve, no flow was observed until a certain forward fluidic pressure was reached. This experiment was done for two different valve closing pressure settings, 25 kPa and 35 kPa. At 25 kPa valve closing pressure, the valve was able to hold the forward fluidic pressure up to 40 kPa without leaking and beyond that, the valve started to leak (**Figure S2D**, white dots). At 35 kPa valve closing pressure, the valve was able to hold the forward fluidic pressure up to 60 kPa and beyond that point, the valve leaked (**Figure S2E**, white dots).

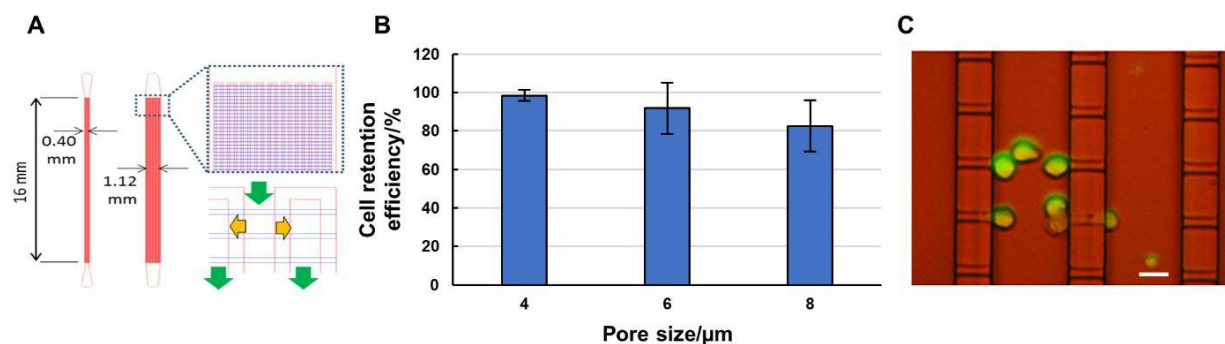


Figure S3. Efficiency of cell retention in the imaging module. (A) General design of the imaging module populated with 2,400 (narrow) and 7,200 (wide) cell retaining pores. (B) Cell retention efficiencies of 4, 6, and 8 μm pore-sized imaging modules. Retention efficiencies were calculated using the number of cells retained in the imaging module and the number of cells in the effluent (n = 3). (C) SKBR3 cells passing through the 6 μm pore imaging module. The scale bar represents 15 μm.

Efficiency of cell retention in the imaging module. Imaging modules contained either 2,400 or 7,200 cell retaining pores and were comprised of two independent fluidic networks (Figure S3A). SKBR3 cells were stained with Calcein and hydrodynamically introduced into the imaging module with different pore sizes (4, 6 and 8 μm) at 20 $\mu\text{L}/\text{min}$ while collecting the effluent. Cell retention efficiencies were determined based on the number of trapped cells in the imaging module and the number of cells in the effluent (Figure S3B). The highest efficiency of cell retention was observed in imaging modules that had 4 μm pore sizes ($98.4 \pm 2.8\%$, $n = 3$) and the lowest cell retention efficiency was observed in 8 μm pore devices ($82.6 \pm 13.3\%$, $n = 3$). SKBR3 cells are $\sim 12 \mu\text{m}$ in diameter⁷ and the cells can escape from 6 and 8 μm pores (Figure S3C) due to the deformability of the cell caused by the fluidic pressure.⁸

Valve Control Steps. Major valve control steps associated with the SMART-Chip when processing a liquid biopsy sample for CTCs are pictured in **Figure S4**. The liquid biopsy sample, in this case whole blood, entered into the cell isolation module with the effluent directed towards the waste reservoir (**Figure S4A**). BSA/PBS was then shuttled into the cell isolation module and finally towards the waste reservoir (**Figure S4B**). After the post selection wash, the cell isolation module was exposed to blue light, which photoreleased the enriched cells and the released cells were directed through the impedance and imaging modules by hydrodynamically introducing Trisglycine buffer through the SMART-Chip (**Figure S4C**). The retained cells within the imaging module were then stained and immunophenotyped (**Figure S4D**). Valves were computer controlled to open/close appropriately during all processing steps for precise fluidic operation in an automated fashion

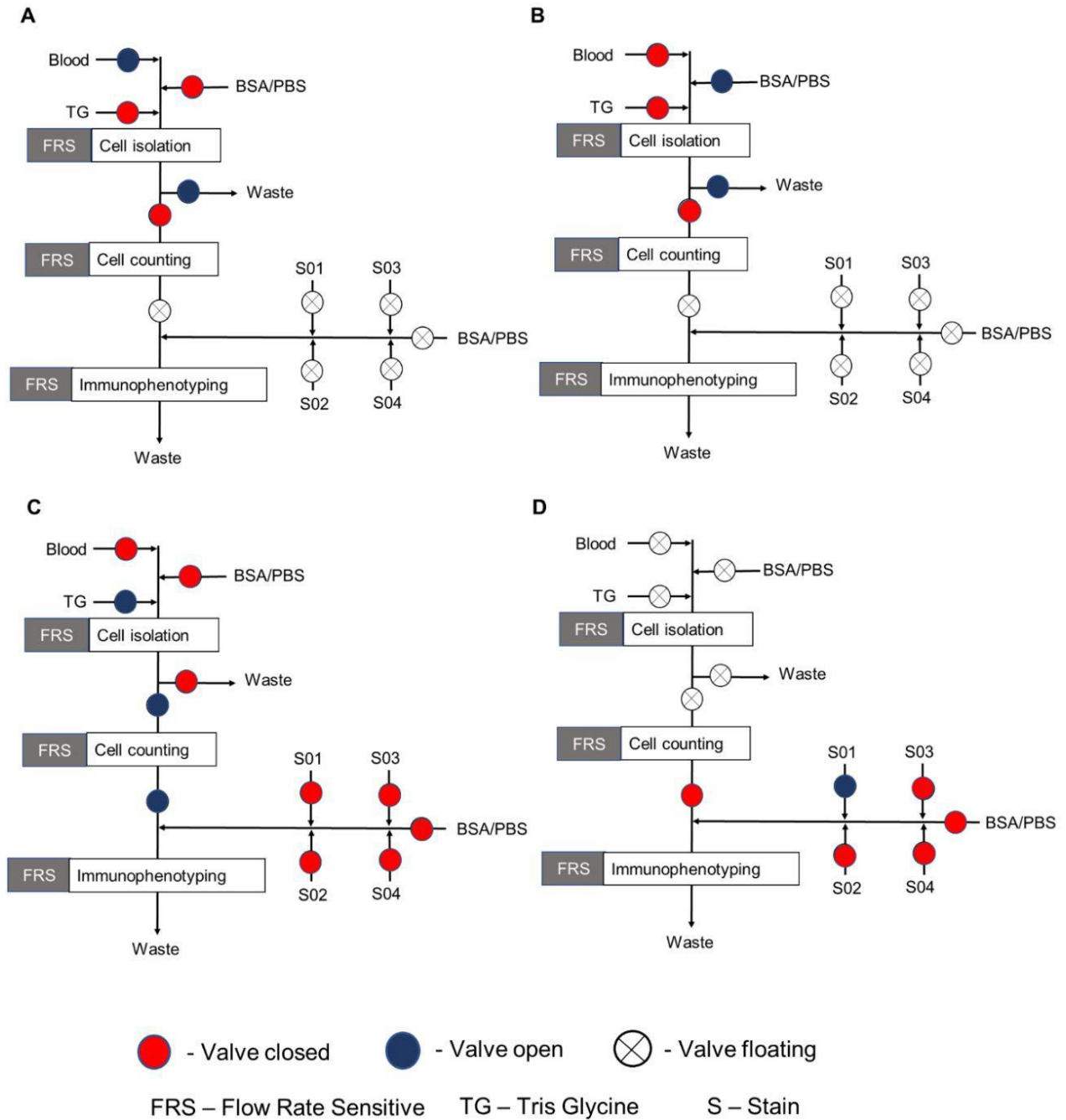


Figure S4. Major valve control steps of the SMART-Chip. **(A)** Whole blood processing, **(B)** post-selection wash with 0.5% BSA/PBS, **(C)** impedance cell counting, and **(D)** immunophenotyping the cells trapped in the imaging module.

Testing of SMART-Chip using SKBR3 CTC surrogates. The ability to analyze CTCs using the SMART-Chip was evaluated by seeding SKBR3 cells as CTC surrogates into whole blood from a healthy donor. Surface antigen expression of the SKBR3 cells were analyzed by flow cytometry and compared with an isotype control. The EpCAM expression of SKBR3 cells were found to be higher than the IgG control (**Figure S5A**). We quantified the cellular EpCAM expression by comparing their fluorescence signatures to Antibody Binding Capacity beads; SKBR3 cells had ~1.4 million EpCAM receptors on their surfaces.

The CTC selection module was decorated with anti-EpCAM mAbs via PC linkers. Hoechst stained SKBR3 cells were spiked into healthy donor blood and affinity enriched using the CTC selection module (**Figure S5B**). The fluorescence seen in the microchannels was due to the coumarin PC linker. Affinity enriched SKBR3 cells were photoreleased using blue-light from an LED and directed towards the impedance module for enumeration. We detected 110 impedance signals (7× higher than noise) and all signals had a positive polarity (100% viable cells; **Figure S5C**). After the impedance module, the cells were directed to the imaging module and immunostained using different fluorescent markers (**Figure S5D**). SKBR3 cells are epithelial breast cancer cells and stained DAPI(+), anti-CD45(-) and anti-Cytokeratin(+) as expected.

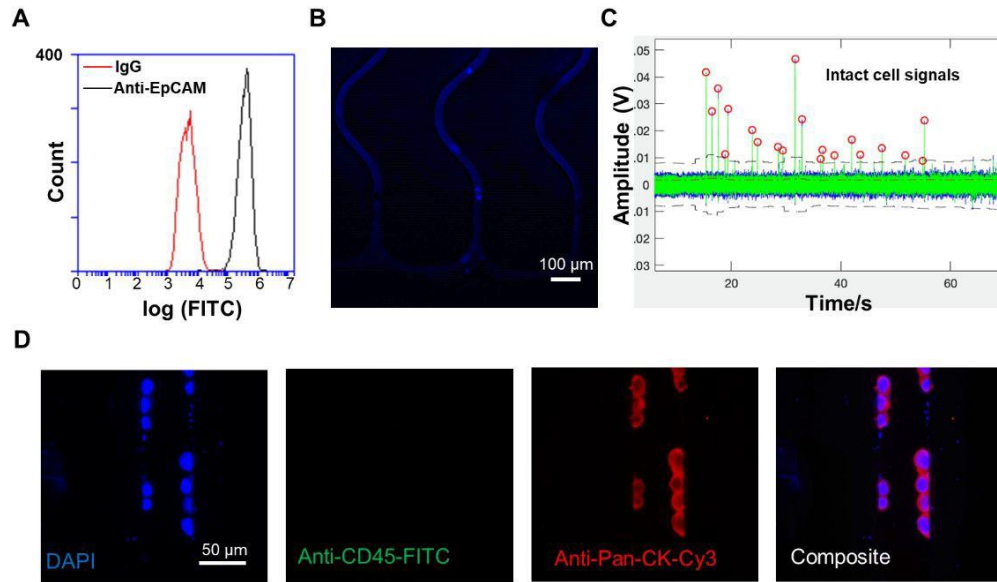


Figure S5. SKBR3 cells were affinity selected and photoreleased for enumeration, viability assessment, and immunophenotypic identification. **(A)** SKBR3 cells were tested for surface EpCAM expression by flow cytometry. Cells were labeled with FITC-conjugated primary antibodies and comparison to the results of a FITC-labeled isotype control. **(B)** Hoechst-stained SKBR3 cells were affinity selected in the CTC selection module by Anti-EpCAM mAbs immobilized to the module's surfaces using the PC linker. **(C)** Photoreleased SKBR3 cells were directed towards the imaging module while recording impedance signals. Part of the impedance trace is displayed. **(D)** SKBR3 cells were physically trapped in the imaging module against the pore structures and immunostained using anti-CD45-FITC and anti-pan-CK-Cy3. Images were taken using a 40X objective.

SMART-Chip- Clinical sample processing. Blood samples obtained from two colorectal cancer patients, and one pancreatic ductal adenocarcinoma (PDAC) patient were processed using the SMART-Chip. Anti-EpCAM antibodies were used for the affinity selection. Affinity captured CTCs were photo-released and directed towards the impedance module and imaging module. Impedance signals were collected ($7\times$ higher than noise) and Hoechst 33342, anti-CD45-FITC and anti-Pan-CK-Cy3 were used to stain physically trapped CTCs in the imaging module. All the data were summarized in the **Table S1**.

Table S1. SMART-Chip clinical sample processing data.

Cancer type	Patient ID	CTCs in imaging module	WBCs in imaging module	Positive impedance signals	Negative impedance signals
CRC	1	9	3	7	0
	2	4	0	0	2
PDAC	3	6	2	4	3

We processed 2 mL of blood in the SMART-Chip and observed 0-3 WBCs (DAPI(+), anti-CD45(+) and anti-Cytokeratin(-)) in the imaging module. The high purity of the fraction is due to the high shear during blood processing (40 dynes per cm²) and the post-selection wash (13 dynes per cm²). These shear did not affect to the antibody-antigen interactions.⁹⁻¹⁰

References

1. M Weerakoon-Ratnayake, K.; Vaidyanathan, S.; Larkey, N.; Dathathreya, K.; Hu, M.; Jose, J.; Mog, S.; August, K.; Godwin, A. K.; L Hupert, M., Microfluidic Device for On-Chip Immunophenotyping and Cytogenetic Analysis of Rare Biological Cells. *Cells* **2020**, *9* (2), 519.
2. Pahattuge, T. N.; Jackson, J. M.; Digamber, R.; Wijerathne, H.; Brown, V.; Witek, M. A.; Perera, C.; Givens, R. S.; Peterson, B. R.; Soper, S. A., Visible photorelease of liquid biopsy markers following microfluidic affinity-enrichment. *Chemical Communications* **2020**, *56* (29), 4098-4101.
3. Zhang, W.; Lin, S.; Wang, C.; Hu, J.; Li, C.; Zhuang, Z.; Zhou, Y.; Mathies, R. A.; Yang, C. J., PMMA/PDMS valves and pumps for disposable microfluidics. *Lab on a Chip* **2009**, *9* (21), 3088-3094.

4. Wong, K. H.; Tessier, S. N.; Miyamoto, D. T.; Miller, K. L.; Bookstaver, L. D.; Carey, T. R.; Stannard, C. J.; Thapar, V.; Tai, E. C.; Vo, K. D., Whole blood stabilization for the microfluidic isolation and molecular characterization of circulating tumor cells. *Nature communications* **2017**, *8* (1), 1-11.
5. Huang, S.; He, Q.; Hu, X.; Chen, H., Fabrication of micro pneumatic valves with double-layer elastic poly (dimethylsiloxane) membranes in rigid poly (methyl methacrylate) microfluidic chips. *Journal of Micromechanics and Microengineering* **2012**, *22* (8), 085008.
6. Kim, J.; Kang, M.; Jensen, E. C.; Mathies, R. A., Lifting gate polydimethylsiloxane microvalves and pumps for microfluidic control. *Analytical chemistry* **2012**, *84* (4), 2067-2071.
7. Liu, Z.; Lee, Y.; hee Jang, J.; Li, Y.; Han, X.; Yokoi, K.; Ferrari, M.; Zhou, L.; Qin, L., Microfluidic cytometric analysis of cancer cell transportability and invasiveness. *Scientific reports* **2015**, *5*, 14272.
8. Kuo, J. S.; Zhao, Y.; Schiro, P. G.; Ng, L.; Lim, D. S.; Shelby, J. P.; Chiu, D. T., Deformability considerations in filtration of biological cells. *Lab Chip* **2010**, *10* (7), 837-42.
9. Adams, A. A.; Okagbare, P. I.; Feng, J.; Hupert, M. L.; Patterson, D.; Göttert, J.; McCarley, R. L.; Nikitopoulos, D.; Murphy, M. C.; Soper, S. A., Highly efficient circulating tumor cell isolation from whole blood and label-free enumeration using polymer-based microfluidics with an integrated conductivity sensor. *Journal of the American Chemical Society* **2008**, *130* (27), 8633-8641.
10. Jackson, J. M.; Witek, M. A.; Soper, S. A., Sinusoidal microchannels with high aspect ratios for CTC selection and analysis. *Circulating Tumor Cells: Isolation and Analysis* **2016**, 85-126.